physica status solidi a
www.pss-a.com

Annealing Kinetics of the Interstitial Carbon–Dioxygen Complex in Silicon

Hussein M. Ayedh, Aleksei A. Grigorev, Augustinas Galeckas, Bengt G. Svensson, and Edouard V. Monakhov*

The interstitial carbon-interstitial dioxygen complex (C_iO_{2i}) has a deep state close to the mid bandgap of Si and can be an efficient recombination center. In this work, the annealing kinetics of C_iO_{2i} in p-type, boron doped, Czochralski grown (Cz) silicon are studied. Two sets of samples are irradiated at room temperature (RT) with 1.8 MeV protons to doses of 1×10^{13} cm^{-2} (set A) and 5×10^{13} cm^{-2} (set B). After irradiation, the samples of both sets are pre-annealed at 400 °C for 30 h in order to anneal out the well-known interstitial carbon-interstitial oxygen (C_iO_i) complex and to form the C_iO_{2i} complex. The annealing of C_iO_i and formation of C_iO_{2i} is monitored by deep level transient spectroscopy (DLTS) via observation of the corresponding electronic levels at 0.36 eV and 0.39 eV above the valence band edge (E_V), respectively. The samples are then subjected to isothermal annealing treatments in the temperature range 450–550 °C. The annealing of C_iO_{2i} follows a first order kinetics, exhibiting an activation energy of 2.55 eV, and a pre-exponential factor in the range (2–30) $\times 10^{12}$ s^{-1}. The kinetics and the deduced parameters suggest that C_iO_{2i} anneals out by dissociation rather than diffusion mechanism.

1. Introduction

The evolution of point defect complexes in silicon (Si) during device processing has a significant impact on the electronic and photovoltaic (PV) devices. A prominent and vivid example of the point defect complexes effect on Si device performance is the so-called light-induced-degradation (LID) of Si solar cells that is most likely attributed to a boron-dioxygen complex.[1] Carbon and oxygen are the most common impurities in Si wafers grown by Czochralski technique (Cz-Si) with concentrations of about 10^{16} and over 10^{17} cm^{-3}, respectively. In as grown Si material they are present predominantly as substitutional carbon (C_s) or interstitial oxygen (O_i), and they are not electrically active in these configurations. However, in Si crystals subjected to implantation or irradiation, interstitial carbon (C_i) is generated by the so-called Watkins replacement mechanism, where C_s is kicked out by Si self-interstitials (Si_i) $Si_i + C_s \leftrightarrow C_i$.[2] C_i is stable up to 270 K and becomes mobile at around room temperature (RT), and the mobile C_i can be captured by O_i forming interstitial carbon-interstitial oxygen complex (C_iO_i). C_iO_i is one of the most dominant defects in irradiated Cz-Si and has a deep level at 0.36 eV above the valence band edge (E_V).

The evolution of C_iO_i upon post-irradiation thermal treatments has been studied intensively for decades. In previous deep level transient spectroscopy (DLTS) studies,[3–5] metastable configurations of C_iO_i has been reported during isochronal annealing of irradiated Si in the temperature range 280–360 K. It has been suggested that an intermediate state, referred to as $C_iO_i^*$, appears before the formation of a stable C_iO_i that persists up to 400 °C. Annealing of C_iO_i has also been studied by photoluminescence spectroscopy (PL) via monitoring the so-called C-line at 789 meV.[6,7] It has been observed that during heat treatments at 350–450 °C the annealing of the C-line is accompanied by the formation of the so-called P-line at 767 meV.[6,7] Several luminescence studies have argued that the P-line is associated with carbon- and oxygen-related defects, and most likely to an oxygen dimer bonded to C_i.[6–10] Later, a correlation has been found between P-line and a DLTS peak at E_V +0.39 eV that forms upon annealing of C_iO_i.[11,12] This peak has been tentatively identified as an interstitial carbon–interstitial dioxygen complex (C_iO_{2i}). The annealing of C_iO_i was suggested to occur via dissociation into C_i and O_i, where the released C_i's can be trapped by oxygen dimers (O_{2i}'s) forming the C_iO_{2i} complex.[11]

The O_{2i}'s are expected to be present in oxygen-rich materials with concentrations of about 10^{13}—10^{14} cm^{-3}.[13] The oxygen dimer (O_{2i}) is strongly believed to be involved in the complex defect causing the LID of Si solar cells,[14–17] therefore, the understanding of O_{2i} related complexes is relevant for PV devices. C_iO_{2i} complex has a deep state close to the mid bandgap and can act as an efficient recombination center limiting the minority carrier lifetime and affecting the performance of power devices. C_iO_i was reported in theoretical studies as a deep donor,[18,19] and C_iO_{2i} has electronic properties similar to that of

Dr. H. M. Ayedh, A. A. Grigorev, Dr. A. Galeckas, Prof. B. G. Svensson[†], Prof. E. V. Monakhov
Department of Physics/Center for Materials Science and Nanotechnology
University of Oslo
P.O. Box 1048 Blindern, N-0316 Oslo, Norway
E-mail: hussein.ayedh@smn.uio.no

[†]Deceased June 24, 2018

DOI: 10.1002/pssa.201800986

C_iO_i and is expected to be a deep donor as well.[11,18] This argument may substantiate the importance of C_iO_{2i} as an efficient recombination center.

In the present study, annealing kinetics of C_iO_{2i} complex is elucidated in detail employing DLTS analysis via monitoring the deep level at E_V +0.39 eV. The annealing of C_iO_{2i} follows first order kinetics and the deduced parameters suggest that dissociation is the dominant annealing mechanism.

2. Experimental Section

Two sets of n^+p diodes were prepared on two nominally identical, p-type (boron doped) Cz-Si wafers with resistivity of ≈14 Ω.cm and net carrier concentration about $\approx 1 \times 10^{15}$ cm^{-3} as determined by capacitance-voltage (*C-V*) measurements at RT with a 1 MHz probe frequency. After a standard RCA cleaning, the wafers were wet oxidized at 1150 °C for 20 min to grow ≈300 nm thick SiO_2 layer. Standard photolithography and wet etching using buffered oxide etch (BOE) were then applied to open holes with a diameter of 1500 μm in selected areas on the oxidized surface. The n^+ layers were formed by thermal in-diffusion of phosphorous (P) from a highly concentrated phosphorus silicate solution (Filmtronics P509 spin-on diffusant (SOD)) that was spun on the two wafers at 3000 rpm for 30 s followed by a hot plate baking for 10 min at 220 °C. Rapid thermal processing (RTP) was employed for thermal in-diffusion of P, where the wafers were placed on a SiC-coated graphite susceptor and thermally treated in an Annealsys AS-Micro furnace at 950 °C for 40 s with heating and cooling rates about 50 °C s^{-1} in N_2 atmosphere. After RTP, the remains of the phosphorus diffusant were removed in a boiled ammonia solution, and an HF dip made the samples hydrophobic after a few seconds. The concentration versus depth profile of phosphorus in the fabricated n^+p diodes was measured by secondary ion mass spectrometry (SIMS), and found that the n^+ layer has maximum P concentration of about 10^{20} cm^{-3} and a depth of about 100 nm. The oxygen and carbon concentration in the wafers were 7×10^{17} cm^{-3} and $\leq 2 \times 10^{16}$ cm^{-3}, respectively, as determined by SIMS. Aluminum (Al) Ohmic contacts were deposited by an electron beam evaporator on the front side (n^+ layer) and silver paste was applied on the back side of the samples to form an Ohmic contact. The fabricated n^+p diodes were subjected to annealing at 300 °C for 26 h in N_2 atmosphere.

The two sets of samples were then irradiated with 1.8 MeV protons at RT to doses of 1×10^{13} cm^{-2} for the first set (labelled "A") and 5×10^{13} cm^{-2} for the second set (labelled "B"). After irradiation, the samples were first annealed at 400 °C for multiple steps (30 h in total) in order to ensure complete annealing of C_iO_i and formation of C_iO_{2i}. Isothermal anneals were carried out on the n^+p diodes in a conventional furnace in a dry N_2 ambient for temperatures in the range of 450–550 °C.

C-V and DLTS measurements were employed after each annealing step for characterizing the samples using a refined version of the setup described in Ref. [20]. In DLTS, the reverse bias quiescent voltage was kept at −10 V with pulse voltage to 0 V and a filling pulse width of 50 ms. The DLTS signal was extracted applying a lock-in and a high resolution weighting function, so-called GS4,[21] with different rate windows in the range of (20–640 ms)$^{-1}$. The C_iO_{2i} concentration was monitored via the deep level at E_V +0.39 eV attributed previously to C_iO_{2i},[11] and having a peak position at ≈190 K in DLTS spectra with a rate window of (640 ms)$^{-1}$ for the GS4 weighting functions.

3. Results and Discussion

Figure 1 shows the DLTS spectra for n^+p Si diodes measured after proton irradiation at RT with doses of 1×10^{13} cm^{-2} (set A) and 5×10^{13} cm^{-2} (set B), and after thermal annealing at 400 °C for different durations. Figure 1a displays the DLTS spectra for set A sample, and the dominant peak in the as-irradiated diode is a characteristic signature of the well-known C_iO_i complex and appears to consist of two overlapping peaks. It has been reported previously that after irradiation at RT a precursor state, $C_iO_i^*$, appears and persists up to 50 °C before the transition to the stable C_iO_i state.[3–5]

The samples annealed at 400 °C have only the stable C_iO_i state with a higher amplitude of the DLTS signal. This shows that the intermediate state, $C_iO_i^*$, has been annealed out and

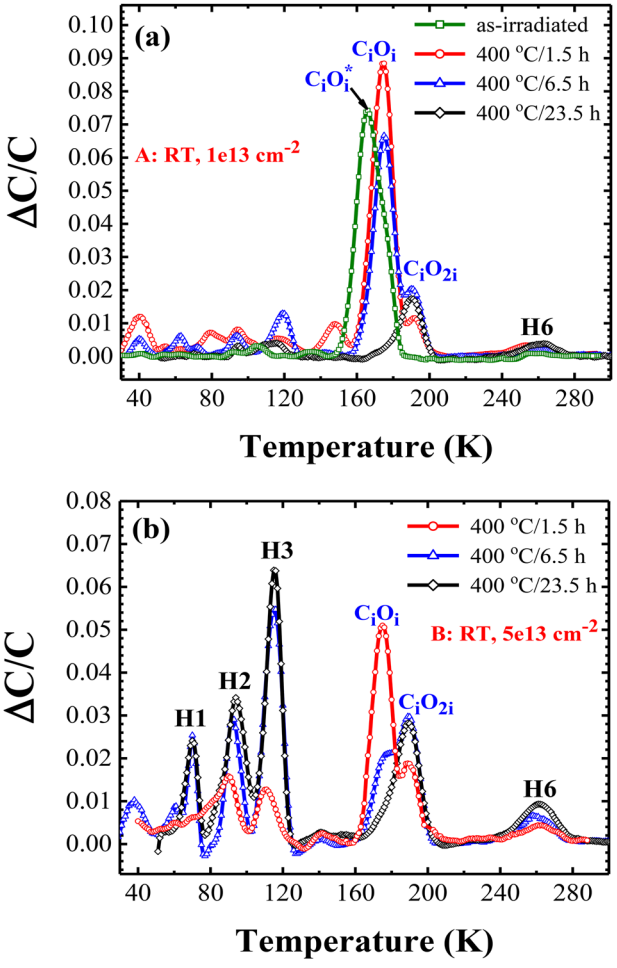

Figure 1. DLTS spectra for samples from set A (a) and set B (b) after irradiation and annealing at 400 °C for 1.5, 6.5, and 23.5 h. Spectra are recorded with rate window (640 ms)$^{-1}$ and GS4 weighting function.

transformed into C_iO_i. After the first annealing step at 400 °C for 1.5 h, a deep level identified previously as C_iO_{2i} emerges.[6–11] Then, after annealing at 400 °C for 6.5 h, C_iO_i is reduced in a correlation with growth of C_iO_{2i}, and after annealing at 400 °C for 23.5 h, C_iO_i is completely annealed out. We should mention here that in a previous study of C_iO_i thermal evolution by Raeissi et al.,[12] a reduction of most of the C_iO_i peak takes place after 1 h annealing at 400 °C, while it required several hours at 400 °C in the present study. This could be attributed to the importance of the revers reaction $C_iO_i \leftrightarrow C_i + O_i$, which can be significant since O_i is the dominant impurity in the material. One can speculate that upon the C_iO_i dissociation the fast migrating C_i can be captured by O_i, C_s, O_{2i} and probably other defects. These interactions are competing, and different impurity content can lead to different apparent annealing rates for C_iO_i. This hypothesis, however, is outside of the scope of the present study and requires a systematic and independent study to be confirmed or ruled out.

The identification of C_iO_i is well established and widely recognized. The strong correlation between C_iO_i annealing and C_iO_{2i} formation (despite the different annealing rate of C_iO_i in different samples) is an additional argument for identification of C_iO_{2i}. One can notice that the correlation between C_iO_i reduction and C_iO_{2i} growth is not one-to-one. This can be expected since O_{2i} is not the only possible trap for migrating C_i's. Besides, the population of O_{2i} may vary during annealing at 400 °C.

The samples from set B have been irradiated with a higher dose, and the as-irradiated samples exhibit significant carrier compensation by the radiation induced defects, which impedes application of DLTS. The amount of the compensation has been measured by *C-V* and exceeds the DLTS applicability limit of around 10%. After the first annealing at 400 °C for 1.5 h, however, the carrier compensation decreases below 10%, and DLTS can be applied. In Figure 1b, the DLTS spectra are displayed for set B sample after multi-step annealing at 400 °C for 1.5, 6.5, and 23.5 h. The major DLTS peaks in the sample after the 400 °C anneal are labeled in Figure 1b as H1, H2, H3, C_iO_i, C_iO_{2i} and H6 with energy level positions at E_V +0.14 eV, E_V +0.20 eV, E_V +0.25 eV, E_V +0.36 eV, E_V +0.39 eV, and E_V + 0.54 eV, respectively. The decrease of $[C_iO_i]$ (bracket denote concentration) with increasing the annealing time is correlated

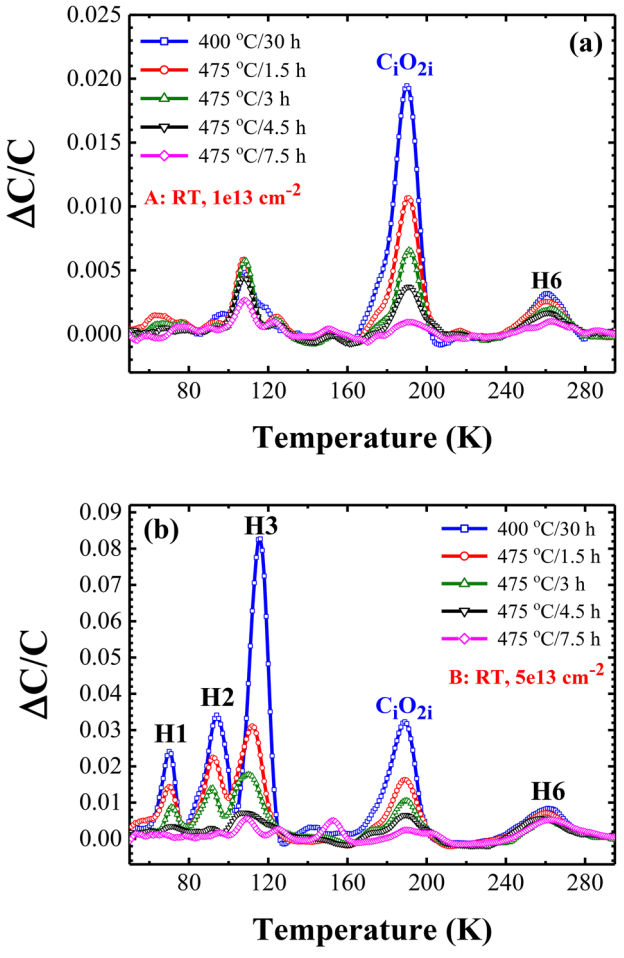

Figure 2. DLTS spectra for samples from set A (a) and set B (b) after annealing at 400 °C for 30 h and at 475 °C for different durations. Spectra are recorded with rate window $(640\ ms)^{-1}$ and GS4 weighting function.

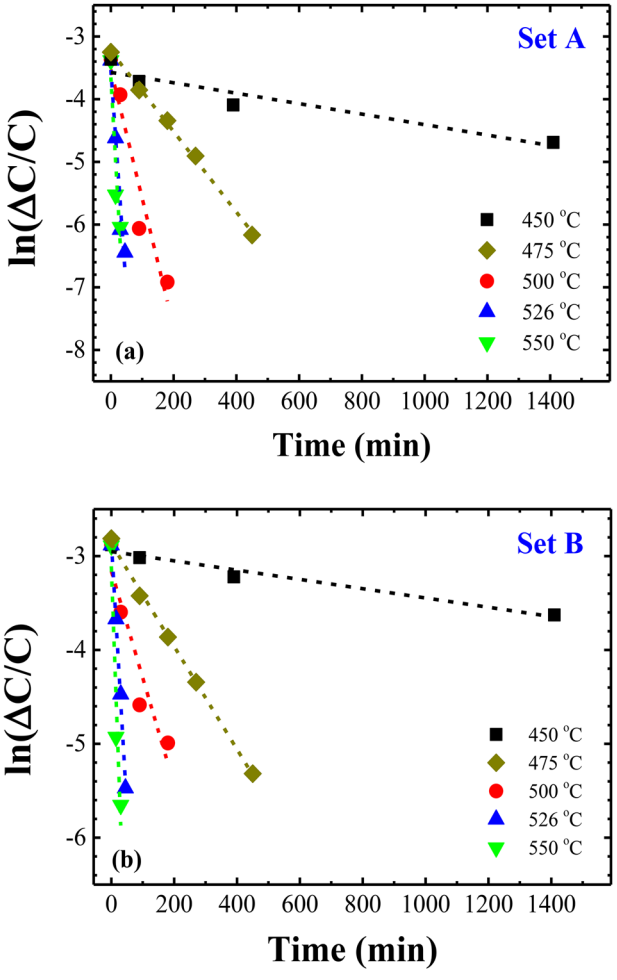

Figure 3. The amplitude of C_iO_{2i} DLTS peak versus annealing time during isothermal annealing at 450, 475, 500, 525, and 550 °C for samples from set A (a) and set B (b).

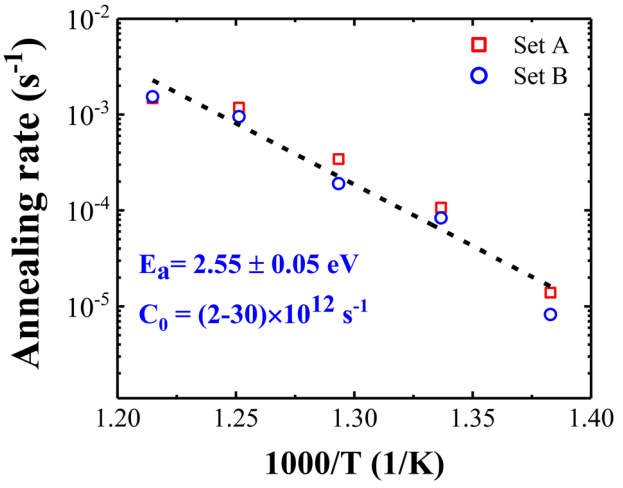

Figure 4. Arrhenius plot for the annealing rate of C_iO_{2i} in samples from set A and set B.

with the C_iO_{2i} formation in a similar way as for set A sample in Figure 1a. In this study, we focus on the annealing kinetics of C_iO_{2i} while the other peaks shown in Figure 1b are outside the scope of this study and will be discussed elsewhere. One should also mention that H1, H2, and H3 lie in the temperature range ($\leq$ 120 K) where a considerable carrier compensation occurs, which makes analysis of these peaks unreliable.

The DLTS spectra of set A and set B diodes after heat treatment at higher temperatures are shown in **Figure 2**a and 2b, respectively. After annealing at 400 °C in total for 30 h, where C_iO_i anneals out and only C_iO_{2i} persists, an isothermal annealing of C_iO_{2i} at 475 °C for different durations are displayed in Figure 2a and 2b. The reduction of $[C_iO_{2i}]$ is observed with increasing the annealing time at 475 °C, and after 7.5 h $[C_iO_{2i}]$ is reduced by about an order of magnitude. The annealing behavior of C_iO_{2i} exhibit similar trend in both set A and set B samples. $[C_iO_{2i}]$ in set A sample is about 70% of that in set B sample even though they underwent irradiation at different doses (set B has doses of five times higher than that for set A). Thus, the formation of C_iO_{2i} upon the annealing of C_iO_i does not follow linear dose dependence. This can be attributed (i) to an intricate balance between O_{2i}'s and other traps for C_i's and (ii) to the depletion of oxygen dimers (O_{2i}'s) which limits the C_iO_{2i} formation. $[O_{2i}]$ is expected to be in the range $10^{13} - 10^{14}$ cm^{-3}, should its concentration follow approximately a $[O_i]^2$ dependence.[13,16] This is in a close agreement with the initial concentration of C_iO_{2i} after the 400 °C anneal which is about $\approx 4 \times 10^{13}$ cm^{-3} in set A and $\approx 6 \times 10^{13}$ cm^{-3} in set B samples. We conclude, thus, that the concentration of C_iO_{2i} in the present samples is limited by the concentration of O_{2i}.

Figure 3 shows the amplitude of C_iO_{2i} peak as a function of the annealing time, at different annealing temperatures for samples from set A (Figure 3a) and set B (Figure 3b). The annealing of C_iO_{2i} follows first order kinetics for both sets of samples. Arrhenius plot for the annealing rates (**Figure 4**) gives an activation energy of 2.55 eV and a pre-factor within a confidence interval of (2–30) $\times 10^{12}$ s^{-1}. The deduced pre-factor is of similar order as the Debye frequency and suggests strongly that the annealing of C_iO_{2i} occurs via a dissociation mechanism.

4. Conclusions

In summary, C_iO_{2i} complex has a deep state close to the mid bandgap and might act as a recombination center for carriers, limiting the minority carrier lifetime and affecting the devices performance. Kinetics annealing studies of the C_iO_{2i} complex in proton irradiated p-type Cz-Si samples have been carried out in the temperature range 450–550 °C. The reduction of C_iO_{2i} concentration versus time follows a first order kinetics, exhibiting an activation energy of 2.55 eV and a pre-factor within a confidence interval of (2–30) $\times 10^{12}$ s^{-1}. The deduced pre-factor suggests that C_iO_{2i} anneals by dissociation.

Acknowledgements

Financial support from the Norwegian Research Council through the research project OxSil (no. 254977) is gratefully acknowledged. The Research Council of Norway is also acknowledged for the support to the Norwegian Micro- and Nano-Fabrication Facility, NorFab, (project no. 245963).

Conflict of Interest

The authors declare no conflict of interest.

Keywords

annealing kinetics, deep level transient spectroscopy, interstitial carbon-dioxygen, oxygen dimer, silicon

Received: December 19, 2018
Revised: March 21, 2019
Published online:

[1] T. U. Naerland, H. Angelskår, E. S. Marstein, *J. Appl. Phys.* **2013**, *113*, 193707.
[2] G. D. Watkins, *Radiation Damage in Semiconductors*, (Ed: P. Baruch), Dunod, Paris **1965**, p. 97.
[3] K. A. Abdullin, B. N. Mukashev, M. F. Tamendarov, T. B. Tashenoy, *Phys. Lett. A* **1990**, *144*, 198.
[4] L. I. Khirunenko, Yu. Pomozov, N. Tripachko, M. Sosnin, A. Duvanskii, L. I. Murin, J. L. Lindström, S. B. Lastovskii, L. F. Makarenko, V. P. Markevich, A. R. Peaker, *Solid State Phenom* **2005**, *108-109*, 261.
[5] L. I. Khirunenko, M. G. Sosnin, Yu. V. Pomozov, L. I. Murin, V. P. Markevich, A. R. Peaker, L. M. Almeida, J. Coutinho, V. J. B. Torres, *Phys. Rev. B* **2008**, *78*, 155203.
[6] G. Davies, R. C. Newman, *Handbook on Semiconductors*, Vol. *3*, (Eds: T. S. Moss, S. Mahajan). Elsevier, Amsterdam **1994**, p. 1557.
[7] G. Davies, S. Hayama, L. Murin, R. Krause-Rehberg, V. Bondarenko, A. Sengupta, C. Davia, A. Karpenko, *Phys. Rev. B* **2006**, *73*, 165202.
[8] W. Kurner, R. Sauer, A. Dornen, K. Thonke, *Phys. Rev. B* **1989**, *39*, 13327.
[9] N. Fukuoka, K. Atobe, M. Honda, *Jpn. J. Appl. Phys.* **1990**, *29*, 1625.
[10] O. O. Awadelkarim, A. Henry, B. Monemar, J. L. Lindström, Y. Zhang, J. W. Corbett, *Phys. Rev. B* **1990**, *42*, 5635.
[11] N. Ganagona, B. Raeissi, L. Vines, E. V. Monakhov, B. G. Svensson, *Phys. Status Solidi C* **2012**, *9*.

[12] B. Raeissi, N. Ganagona, A. Galeckas, E. V. Monakhov, B. G. Svensson, *Solid State Phenom*. **2014**, *205-206*, 224.
[13] L. I. Murin, T. Hallberg, V. P. Markevich, J. L. Lindström, *Phys. Rev. Lett*. **1998**, *80*, 93.
[14] J. Schmidt, *Solid State Phenom*. **2004**, *95-96*, 187.
[15] V. V. Voronkov, R. Falster, *J. Appl. Phys*. **2010**, *107*, 053509.
[16] L. I. Murin, E. A. Tolkacheva, V. P. Markevich, A. R. Peaker, B. Hamilton, E. Monakhov, B. G. Svensson, J. L. Lindström, P. Santos, J. Coutinho, A. Carvalho, *Appl. Phys. Lett*. **2011**, *98*, 182101.
[17] V. V. Voronkov, R. Falster, A. V. Batunina, D. Macdonald, K. Bothe, J. Schmidt, *Energy Procedia* **2011**, *3*, 46.
[18] C. P. Ewels, R. Jones, S. Öberg, *Early Stages of Oxygen Precipitation in Silicon*, (Ed: R. Jones), Kluwer Academic Press, Ser. 3 **1996**, p. 17.
[19] J. Coutinho, R. Jones, P. R. Briddon, S. Öberg, L. I. Murin, V. P. Markevich, J. L. Lindström, *Phys. Rev. B* **2001**, *65*, 014109.
[20] B. G. Svensson, K.-H. Rydén, B. M. S. Lewerentz, *J. Appl. Phys*. **1989**, *66*, 1699.
[21] A. A. Istratov, *J. Appl. Phys*. **1997**, *82*, 2965.